International Journal of Heat and Mass Transfer 222 (2024) 125205

Contents lists available at ScienceDirect

International Journal of Heat and Mass Transfer

journal homepage: www.elsevier.com/locate/ijhmt

# Arbitrary-shape transformation multiphysics cloak by topology optimization

Zhan Zhu [a], Zhaochen Wang [a], Tianfeng Liu [a], Bin Xie [b], Xiaobing Luo [a], Wonjoon Choi [c,*], Run Hu [a,d,*]

[a] School of Energy and Power Engineering, Huazhong University of Science and Technology, Wuhan 430074, China
[b] State Key Laboratory of Digital Manufacturing Equipment and Technology, Huazhong University of Science and Technology, Wuhan 430074, China
[c] School of Mechnical Engineering, Korea University, Seoul 02841, Republic of Korea
[d] Key Laboratory of Thermal Science and Power Engineering of Ministry of Education, Tsinghua University, Beijing 100084, China

ARTICLE INFO

*Keywords:*
Thermal metamaterial
Transformation theory
Multi-physics topology optimization
Multiphysics metamaterial
3D printing

ABSTRACT

Transformation theory has enabled the booming development of metamaterials which have offered powerful capability to control different physical fields, and the remaining challenges lie in the robust design of extremely anisotropic material parameters. Such challenges surge for multiphysics metamaterials is more difficult though not impossible. Previous studies on multiphysics metamaterials have neither established a general framework nor tackled the limited shape adaptivity beyond the scattering cancellation technique. Here, those challenges are successfully addressed by the transformation multiphysics cloak (TMC), through which a general design framework is established under the discretion-and-assembly strategy with topology optimization. As proof-of-concept, we design an arbitrary-shape TMC to achieve the simultaneous cloaking of heat and electric current transiently and steadily, which is validated by both numerical simulations and experimental measurements. The proposed method may trigger unprecedented development of multiphysics metamaterials in other physical fields with integration of more functionalities, shape adaptivity, and application scenarios.

## 1. Introduction

Since the birth of transformation optics in 2006, metamaterials have emerged and soared with extraordinary properties beyond the nature-occurring materials to enable multifarious functionalities and promising applications in different disciplines, including electromagnetics and optics [1,2], acoustics [3–5], thermotics [6–11], mechanics [12–14] etc. The essence of these extraordinary properties and novel functionalities lies in the robust design and fabrication of extremely anisotropic material parameters originated from the coordinate transformation in the transformation theory. The naturally existing homogeneous materials usually fail to achieve such extreme anisotropy of material parameters, hence the artificially structured materials, a.k.a. metamaterials are strongly demanded to meet the severe requirements of anisotropic material properties. Among these novel functionalities of metamaterials, the milestone — invisible cloak, which renders objects invisible from the external observers, has attracted the most scientific attentions since its birth. In 2006, the seminal electromagnetic invisible cloak was first designed by the transformation optics theory [1] and experimentally validated subsequently, which triggers the significant development of metamaterials and open avenues for manipulating electromagnetics and optics. Therewith, the invisible cloak is extended to acoustic cloak [3–5], thermal cloak [15–19], mechanical cloak [20,21], matter wave cloak [22–24] and so on. However, most of these cloaks only consider one particular physical field rather than multiphysics fields. For example, the designed thermal cloak can only manipulate heat flux, and the designed electric cloak can only control electric current. As shown in Fig. 1a and b, the thermal cloak and electric cloak work well on manipulating the heat flux and electric current independently. If we directly apply a thermal cloak in the electric field in Fig. 1c, the electric field will be distorted more or less, and vice versa. This is because the key parameters in each field, i.e. the thermal conductivity $\kappa$ and the electric conductivity $\sigma$, are not coupled or even considered when we design an electric or a thermal cloak respectively. But if we couple $\kappa$ and $\sigma$, the multiphysics cloak, as shown in Fig. 1d, can maintain the desired functionalities in multiphysics fields simultaneously as ideal as those in the single physical field. Multiphysics metamaterials can exert their abilities more effectively in the real scenario,

* Corresponding authors.
*E-mail addresses:* wojchoi@korea.ac.kr (W. Choi), hurun@hust.edu.cn (R. Hu).

https://doi.org/10.1016/j.ijheatmasstransfer.2024.125205
Received 16 September 2023; Received in revised form 26 December 2023; Accepted 14 January 2024
Available online 19 January 2024

since the real scenario always involves complex multiphysics fields. On the contrary, the applicability of single-physical-field metamaterials is relatively poor. It is necessary to propose a computational framework for the precise design of multiphysics metamaterials. However, The coupling of $\kappa$ and $\sigma$ is not easy as $\kappa$ and $\sigma$ should be considered simultaneously. Therefore, it is a big challenge to design a multiphysics cloak that can work well in multiphysics fields. To achieve multiphysics metamaterials, not only the governing equations had better be at the same form to simplify design, but also the parameters should be coupled during the design and fabrication process. Though challenging, multiphysics metamaterials is profoundly significant as they will definitely broaden the current understanding of metamaterials and enable the feasible manipulation of multiphysics fields with a single device. So far, there are very limited multiphysics metamaterials in terms of manipulating heat flux and electric current [25–32] both theoretically and experimentally. In 2014, Ma et al. demonstrated the experimental thermal-electric cloak [28] with an annular shell based on the scattering cancellation techniques [33–35]. The scattering cancellation technique, originated from the source-free plane wave solution to the Laplace equations, only designs global effective properties for regular shapes rather than designing local properties, which limits the functionality and shape of metamaterials. Therefore, it is rather important to develop a general method for the design of multiphysics metamaterials breaking the limitations of the scattering cancellation technique. Topology optimization, as a mathematical method to optimize material distribution within a given design area based on given load conditions, constraints, has been widely studied to apply in designing multiphysics metamaterials [36–40]. Most of them [36–38] design the global topological structure with the objective function to minimize the difference the actual physical field and the expected physical field. To obtain stronger local regulation ability, metamaterials based on multiscale optimization was studied [39], the design domain was divided into eight regions, which filled with arrangement of different unit-cell structures. Owing to the difficulty of preparation, most of the researches are lack of experimental validation. To manipulate heat flux and electric current preciously and locally, we propose a design framework, including the discretion-and-assembly strategy and multi-physics topology optimization aiming to achieve the target properties, which advances in stronger local control ability of heat flux/electric current, more flexibility in shape selection and more robustness under different working conditions.

In this paper, we present a general roadmap to design transformation multiphysics cloak (TMC) to enable the simultaneous cloaking of heat flux and electric current with a single device. We design the TMC by coupling the transformation optics and multi-physics topology optimization techniques based on the properties, and fabricate the experimental samples by three-dimensional (3D) printing. Both finite-element simulations and experiments are conducted to validate the multiphysical cloaking performance.

## 2. Materials and methods

The whole design procedure of the arbitrary-shape TMC is shown in Fig. 2. We apply the transformation theory to design the arbitrary-shape TMC and calculate the theoretical thermal and electric conductivity

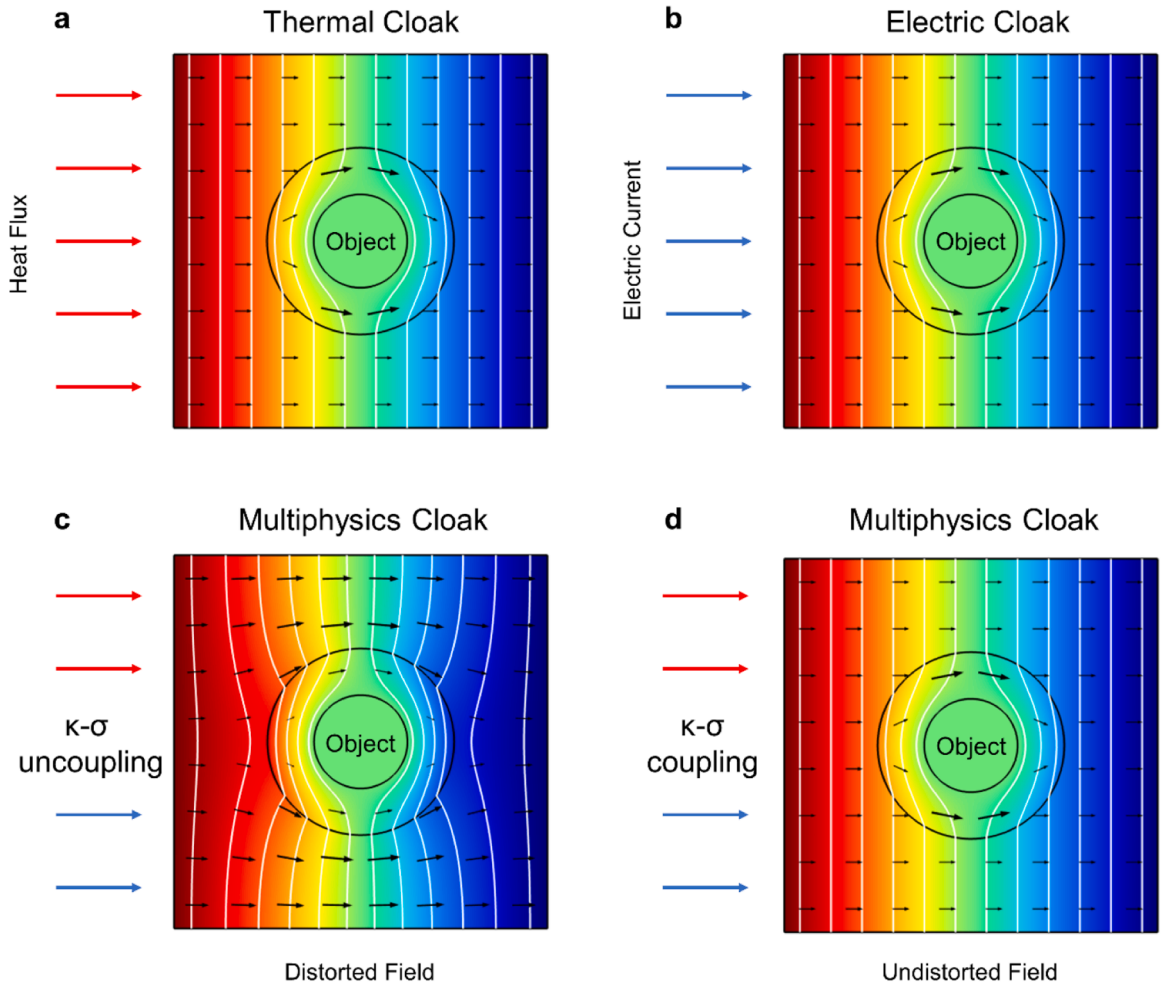


**Fig. 1.** Implementation of TMC. (a) Thermal cloak can only manipulate heat flux. (b) Electric cloak can only manipulate electric current. (c) Failure of multiphysics cloak without coupling $\kappa$ and $\sigma$. (d) Successful implementation of TMC with coupling $\kappa$ and $\sigma$.

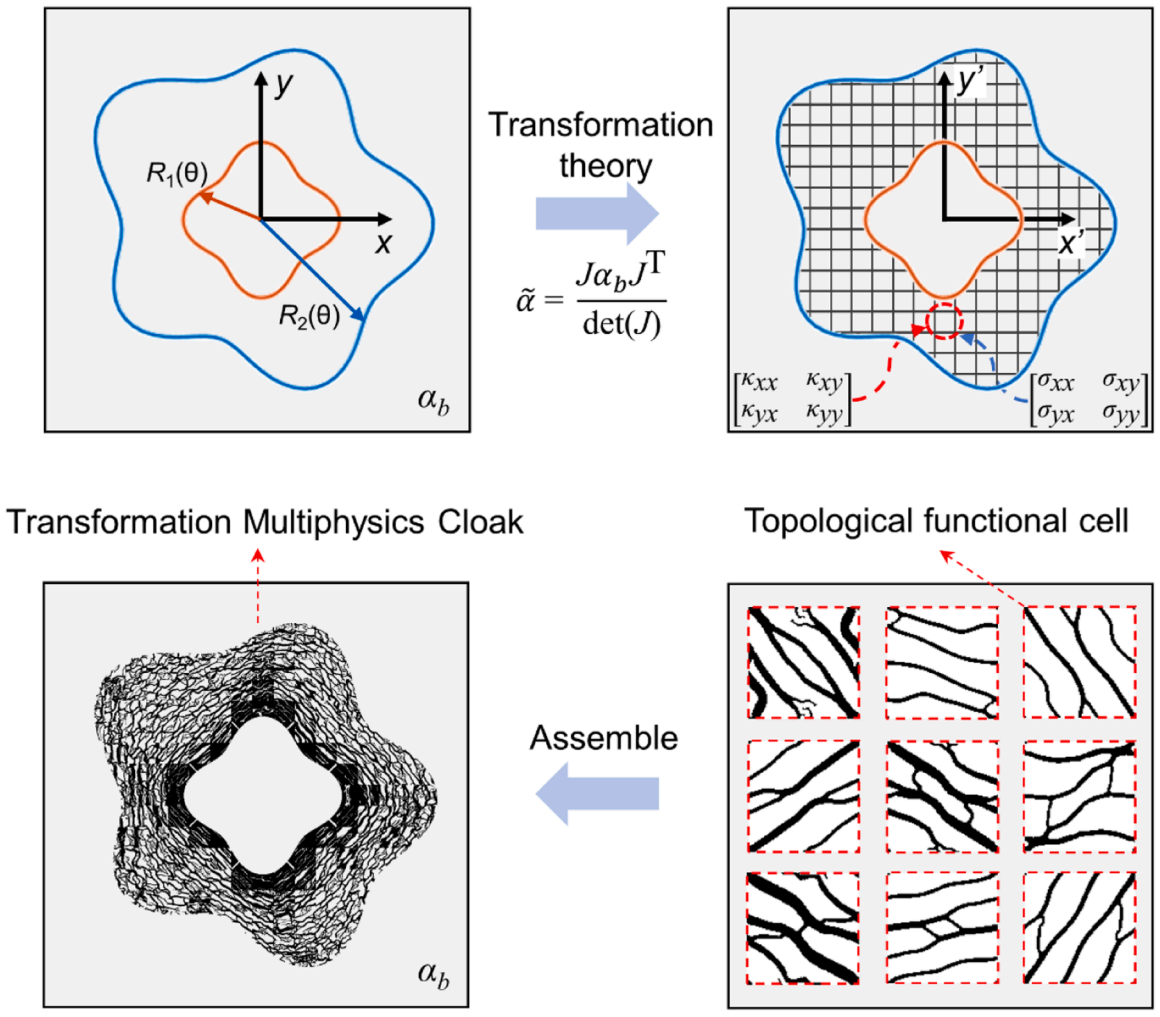


**Fig. 2.** Design procedure of an arbitrary-shape multiphysics cloak. First, Divide the design region into discrete square cells. Second, calculate the target $\kappa$ and $\sigma$ of each cell and obtain the topological function cell by topology optimization. Third, assemble them into the whole multiphysics cloak.

tensors. Beginning with transformation optics, the transformation theory has been extended to many other disciplines, such as acoustics, elastics, thermotics, DC electric current, etc. [41–46]. With the invariance of the governing equation in coordinate transformation, the transformation theory can be similarly applied to the thermal and electric fields since they have the same form of the governing equations. To design the arbitrary-shape TMC, we map the entire region $r \le R_2(\theta)$into the annular one $R_1(\theta') \le r' \le R_2(\theta')$, as

$$\begin{cases} r' = \dfrac{R_2(\theta) - R_1(\theta)}{R_2(\theta)} r + R_1(\theta) \\ \theta' = \theta \end{cases} \tag{1}$$

The corresponding conductivity ($\tilde{\sigma}$ and $\tilde{\kappa}$) $\tilde{\alpha}$ in real space can be calculated as $\tilde{\alpha} = J\alpha_b J^T/\det(J)$, where $J$ is the Jacobian matrix of the coordinate transformation, $\alpha_b$ is the conductivity of the background (as shown in Fig. 2) and $\det(J)$ is the determinant of the matrix $J$. The Jacobian matrix $J$ in Cartesian coordinate system can be deduced from coordinate transformation step by step, i.e. $(x,y)\to(r,\theta)\to(r',\theta')\to(x',y')$. Accordingly, the conductivity $\tilde{\alpha}$ for the annular region $R_1(\theta') \le r' \le R_2(\theta')$ is

$$\begin{cases} \tilde{\alpha} = \begin{bmatrix}\tilde{\alpha}_{11} & \tilde{\alpha}_{12}\\ \tilde{\alpha}_{21} & \tilde{\alpha}_{22}\end{bmatrix} = \alpha_b \begin{bmatrix}\cos\varphi & -\sin\varphi\\ \sin\varphi & \cos\varphi\end{bmatrix} \begin{bmatrix}(\alpha_{11})_{r\theta} & (\alpha_{12})_{r\theta}\\ (\alpha_{21})_{r\theta} & (\alpha_{22})_{r\theta}\end{bmatrix} \begin{bmatrix}\cos\varphi & -\sin\varphi\\ \sin\varphi & \cos\varphi\end{bmatrix}^T \\ (\alpha_{11})_{r\theta} = \dfrac{(r' - R_1(\theta'))^2 + C^2}{r'(r' - R_1(\theta'))} \\ (\alpha_{12})_{r\theta} = (\alpha_{21})_{r\theta} = \dfrac{C}{r' - R_1(\theta')} \\ (\alpha_{22})_{r\theta} = \dfrac{r'}{r' - R_1(\theta')} \\ C = \dfrac{R_1(\theta')(r' - R_1(\theta'))\dfrac{dR_2(\theta')}{d\theta'} - R_2(\theta')(r' - R_2(\theta'))\dfrac{dR_1(\theta')}{d\theta'}}{R_2(\theta')(R_2(\theta') - R_1(\theta'))} \end{cases} \tag{2}$$

where $\varphi$is the azimuth coordinate. From Eq. (2), the corresponding conductivity is inhomogeneous concerned with the geometric dimension and the background conductivities, and it is rather challenging to fabricate them with naturally-occurring materials. For this end, we propose a discretion-and-assembly strategy to design and fabricate the TMC with anisotropic conductivity tensors based on multi-physics topology optimization. Note that topology optimization is a numerical computation method that can obtain the required properties by optimizing volume fractions and distributions of different materials in a

fixed area, we employ multi-physics structural topology optimization to achieve the desired thermal and electric conductivities simultaneously. We divide the metamaterials region into discrete square cells, where each cell takes the local thermal and electric conductivities of the central point as optimization objective to input the optimization procedure. In topology optimization, each square cell is meshed into a certain number of finite elements and each element is assigned a density continuously ranging from 0 to 1, which is the design variable of topology optimization. The mapping relation between the density and the material properties is defined by modified solid isotropic material with penalization (SIMP) scheme as $\alpha(\rho_i) = \alpha_{material1} + \rho_i^p(\alpha_{material2} - \alpha_{material1})$ [47], where $p$ is the penalty coefficient and $\rho_i$ is the density of a finite element. From the above formula, it can be concluded that the finite element with density 0 means material 1 and the finite element with density 1 means material 2. Densities other than 0 and 1 are not allowed, since these densities represent other materials that are not defined in the optimization procedure, which should be binarized in the post-processing step. The homogenized $\kappa$ and $\sigma$ will be influenced with the change of densities. To minimize the influence, the binarization threshold of each cell is obtained by binary search method. The initial threshold is set as 0.5, the middle value of 0 and 1, the threshold is updated iteratively with changing the upper bound and the lower bound to make the homogenized properties achieve the original properties as close as possible. After setting reasonable objective function and constraints, the design variable $\rho_i$ can be updated constantly until the optimized material distribution achieves the target properties.

The multi-physics optimization model is formulated as

$$\begin{cases} minC = \dfrac{1}{|\Omega|}\sum_{i=1}^{N}\rho_i \\ s.t.: \boldsymbol{K}_{t,\ e}(\rho_i)\boldsymbol{\Gamma}_{t,e} = \boldsymbol{Q}_{t,e}, \\ G = f(\alpha_{ij},\ \alpha_{input}) = 0,\ (i,j = 1,\ 2) \\ 0 \le \rho_i \le 1,\ i = 1,\ 2\ldots N \end{cases} \tag{3}$$

$$G = \left(\kappa_{11} - \kappa_{11}^{input}\right)^2 \Big/ \kappa_{11}^{input} + \left(\kappa_{22} - \kappa_{22}^{input}\right)^2 \Big/ \kappa_{22}^{input} + \left(\kappa_{12} - \kappa_{12}^{input}\right)^2 + \left(\kappa_{21} - \kappa_{21}^{input}\right)^2 + \left(\sigma_{11} - \sigma_{11}^{input}\right)^2 \Big/ \sigma_{11}^{input} + \left(\sigma_{22} - \sigma_{22}^{input}\right)^2 \Big/ \sigma_{22}^{input} + \left(\sigma_{12} - \sigma_{12}^{input}\right)^2 + \left(\sigma_{21} - \sigma_{21}^{input}\right)^2 \tag{4}$$

The usual topology optimization model aims to obtain the extreme properties with fixed volume fraction, i.e. the objective function involves the properties and the constraint is set as a fixed volume fraction. However, this model does not work well to obtain materials distribution with the target properties. The selection of the fixed volume fraction is totally blind, which may lead to inaccurate optimization results even when the objective function aims to minimize the difference between the actual properties and the target properties [49].

To verify the effectiveness of the model, the histories of the constraint and objective function were plotted in Fig. 3. We take $\begin{bmatrix} 10 & 5 \\ 5 & 13 \end{bmatrix}$ W m$^{-1}$ K$^{-1}$ and $\begin{bmatrix} 15 & 7 \\ 7 & 18 \end{bmatrix} \times 10^5 \Omega^{-1}$ m$^{-1}$ as target properties, PDMS as material 1 ($\kappa_1 = 0.16$ W m$^{-1}$ K$^{-1}$, $\sigma_1 = 0.1\ \Omega^{-1}$ m$^{-1}$) and Cu as material 2 ($\kappa_2 = 400$ W m$^{-1}$ K$^{-1}$, $\sigma_2 = 5.81 \times 10^7\ \Omega^{-1}$ m$^{-1}$). The constraint and objective function show a decreasing trend during the optimization process, which meets the requirements of simultaneously achieving the thermal and electric conductivities. The design variable of four corners in each topological functional cell (TFC) is set as 1 to make sure each cell is connected with each other. In this mathematical model, the design variable $\rho_i$ will be updated with the method of moving asymptotes (MMA) [50]. By introducing moving asymptotes, MMA method transforms the implicit optimization problem into a series of explicitly simpler and strictly convex approximate suboptimization problems. In each iteration step, new design variables are obtained by solving an approximately convex subproblem. The sensitivities of constraint $G$ and objective function $C$ are calculated by differentiating them with respect to the design variable following the adjoint method.

$$\frac{\partial G}{\partial \rho_i} = \frac{2\left(\kappa_{11} - \kappa_{11}^{input}\right)}{\kappa_{11}^{input}}\frac{\partial \kappa_{11}}{\partial \rho_i} + \frac{2\left(\kappa_{22} - \kappa_{22}^{input}\right)}{\kappa_{22}^{input}}\frac{\partial \kappa_{22}}{\partial \rho_i} + 2\left(\kappa_{12} - \kappa_{12}^{input}\right)\frac{\partial \kappa_{12}}{\partial \rho_i} + 2\left(\kappa_{21} - \kappa_{21}^{input}\right)\frac{\partial \kappa_{21}}{\partial \rho_i} + \frac{2\left(\sigma_{11} - \sigma_{11}^{input}\right)}{\sigma_{11}^{input}}\frac{\partial \sigma_{11}}{\partial \rho_i} + \frac{2\left(\sigma_{22} - \sigma_{22}^{input}\right)}{\sigma_{22}^{input}}\frac{\partial \sigma_{22}}{\partial \rho_i} + 2\left(\sigma_{12} - \sigma_{12}^{input}\right)\frac{\partial \sigma_{12}}{\partial \rho_i} + 2\left(\sigma_{21} - \sigma_{21}^{input}\right)\frac{\partial \sigma_{21}}{\partial \rho_i} \tag{5}$$

where $f(\alpha_{lm},\ \alpha_{input})$ calculates the difference between the effective conductivity $\alpha_{lm}$ and the target conductivity $\widetilde{\alpha}_{input}$ of each cell. $\boldsymbol{K}_{t,\ e}(\rho_i)$, $\boldsymbol{\Gamma}_{t,e}$ and $\boldsymbol{Q}_{t,e}$ are the global heat/electric conduction matrix, global temperature/potential matrix and global thermal/electric load matrix respectively. $\boldsymbol{K}_{t,\ e}(\rho_i)$, and $\boldsymbol{Q}_{t,e}$ can be quantified by $\boldsymbol{K}_{t,\ e}(\rho_i) = \sum_{i=1}^{N}\boldsymbol{\Lambda}_i$ and $\boldsymbol{Q}_{t,e} = \sum_{i=1}^{N}\boldsymbol{N}\boldsymbol{q}_i^0$, where $\boldsymbol{\Lambda}_i$is the element thermal/electric conductivity matrix calculated by $\boldsymbol{\Lambda}_i = \alpha(\rho_i)\int_{\Omega_i}\left[\left(\frac{\partial \mathbf{N}}{\partial x}\right)^T\left(\frac{\partial \mathbf{N}}{\partial x}\right) + \left(\frac{\partial \mathbf{N}}{\partial y}\right)^T\left(\frac{\partial \mathbf{N}}{\partial y}\right)\right]d\Omega_i$, $\mathbf{N}$ is the shape function and $\Omega_i$ is the area of a finite element. The homogenized thermal/electric conductivity is calculated by the numerical homogenization method, i.e. $\alpha_{ij} = \frac{1}{|\Omega|}\sum_{e=1}^{N}\left(\Delta \mathrm{T}_e^{(i)}\right)^T\alpha_e\Delta \mathrm{T}_e^{(j)}$, where $\Delta \mathrm{T}_e = \mathrm{T}_e^0 - \mathrm{T}_e$ is the temperature difference vector, $\mathrm{T}_e^0$ is the nodal temperature vector under the uniform test heat flow, $\mathrm{T}_e$ is the induced nodal temperature field. Note that the difference between the homogenized conductivity$\alpha_{ij}$ and the target conductivity$\widetilde{\alpha}_{input}$ is set as the constraint rather than the objective function so as to obtain a more precious optimization result [48]. The heuristic formulas of the constraint function $G$ are set as

$$\frac{\partial C}{\partial \rho_i} = \frac{1}{|\Omega|} \tag{6}$$

Each topological functional cell can be optimized to achieve the target conductivity through multi-physics topology optimization. The procedure of the optimization method is as follow: 1) Given initial material distribution, the density of each cell is set as 0.5. 2) The thermal conductivity and electric conductivity of each cell are calculated by numerical homogenization method. Object function is calculated and used to decide if it meets the convergence criterion. If the value of object function meets the convergence criterion, the optimization program ends and outputs the final material distribution. After binarization processing, the final topological structure of each cell is obtained. 3) If the value of object function does not meet the convergence criterion, the design variable needs update iteratively. The sensitivities of object function and constraint are calculated firstly and the design variable is updated by using the method of moving asymptotes (MMA). 4) Iteratively execute step2 and step3 util it achieves the convergence and outputs the final material distribution. Finally, we assemble all the TFCs into the arbitrary-shape TMC. More specifically, the topological

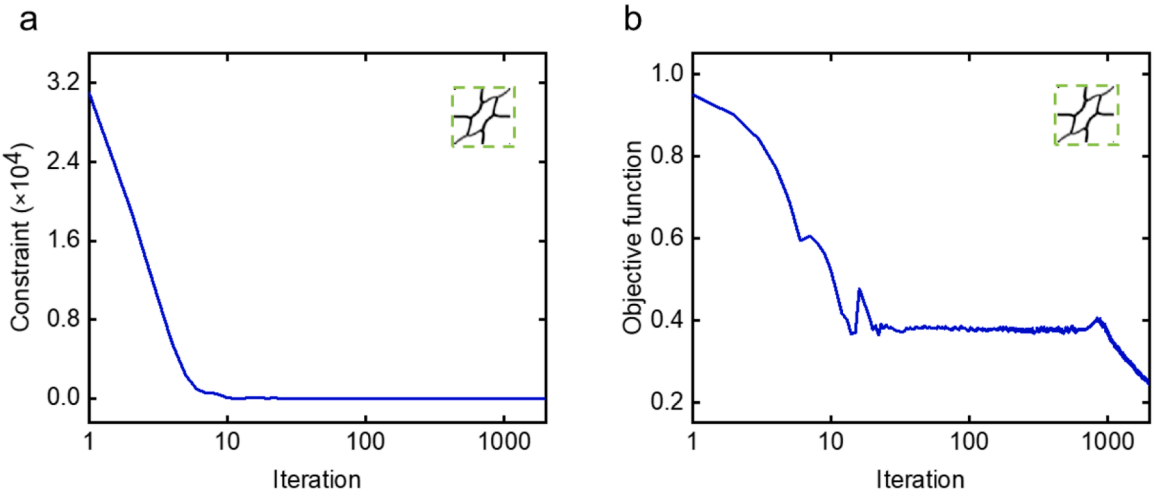


**Fig. 3.** The history of the constraint $G$ and the objective function $C$ during the optimization process.

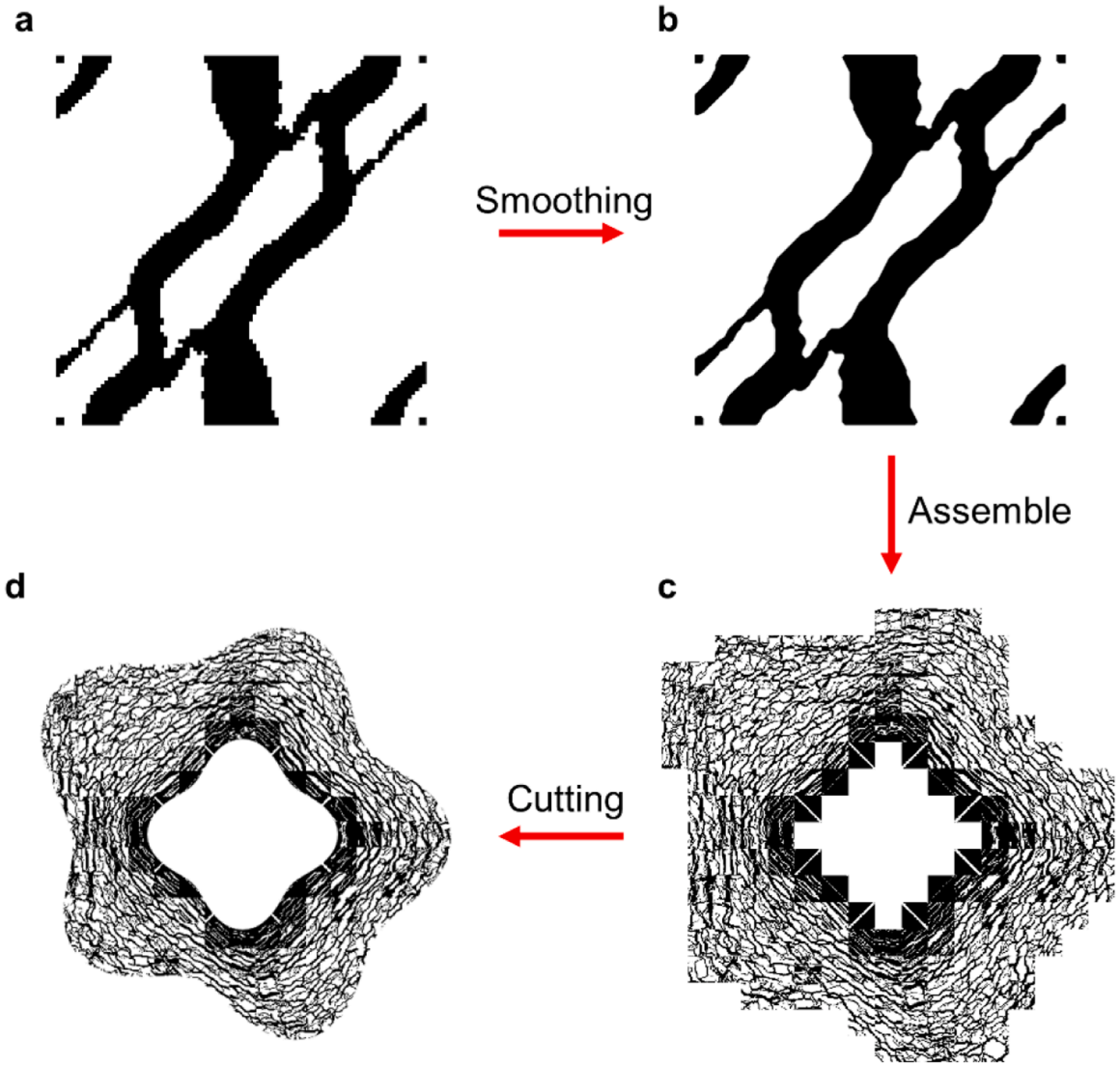


**Fig. 4.** The design process of arbitrary-shape TMC. (a) Optimized structure of a single TFC. (b) Smoothed structure of a single TFC. (c) The structure of TMC by assembling all TFCs. (d) The reprocessed structure of TMC after cutting redundant edges.

structure of each TFC is imported into COMSOL Multiphysics. To make the inner and outer interfaces of multiphysics cloak meet the preset settings, we defined the parameterized curves of them and select the intersection between the original geometric and the curves. Note that the more TFCs in the TMC, the better performance of the TMC as the theoretical transformation theory.

## 3. Results and discussion

We validate the cloaking performance of the designed arbitrary-shape TMC by both FEM simulations and experiments. As for the arbitrary shape of the TMC, two parameterized curves to describe the shape of TMC with respect to azimuth coordinate $\theta$ are set as $R_1(\theta) = 1.25[2\cos(4\theta) + 13]$ mm, and $R_2(\theta) = 2.5[15 + 0.5\sin\theta - \sin(2\theta) - 0.5\cos\theta + 2\cos(5\theta)]$mm. The background is a 125 mm × 125 mm titanium plate with $\kappa = 21.9$ W m$^{-1}$ K$^{-1}$ and $\sigma = 2.6 \times 10^6$ Ω$^{-1}$ m$^{-1}$, which is divided into 25 × 25 TFCs. Further, we mesh each TFC into 100 × 100 square finite elements with dimension of 0.05 mm × 0.05 mm for storing the design variable $\rho_i$. Following above procedure, we can get the TMC structure after assembling all TFCs. The detailed design process is plotted in Fig. 4.

Then, the multiphysics cloaking effect under different linear temperature/potential gradient are simulated with finite-element method (FEM) in Fig. 5. The simulation results show that the external physical fields keep parallel and there is no temperature/potential gradient in the internal physical fields, which means heat flux/electric current bypasses the central cloaking region and keeps its original direction to spread just like the internal object was cloaked. It is seen that the TMC maintains its both thermal cloaking and electric cloaking effects simultaneously under linear temperature/potential gradients with eight different directions, which showcases the robust omnidirectional manipulating of heat flux and electric current with a single device. In addition, we also

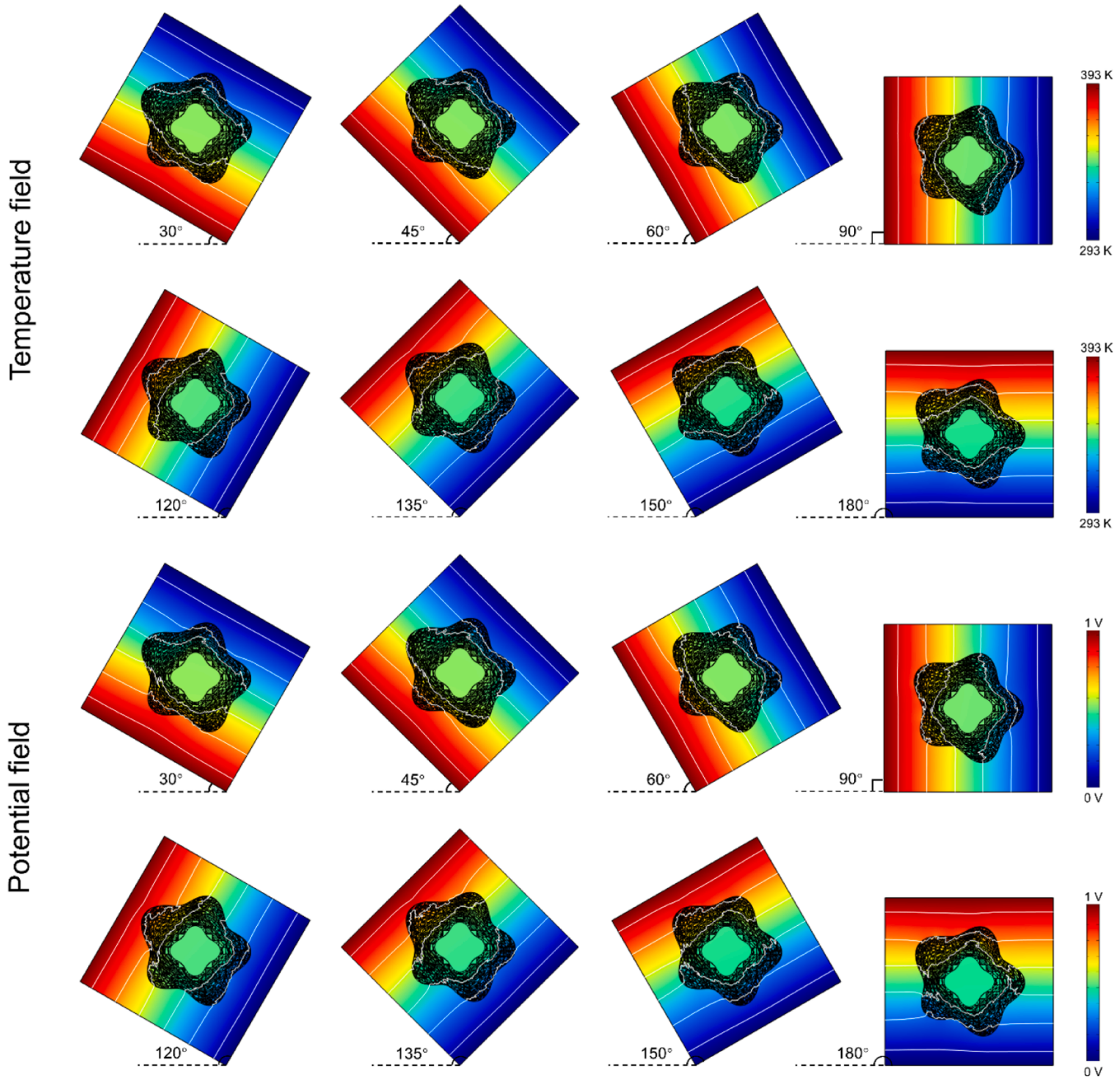


**Fig. 5.** Simulations of the TMC under different temperature/potential gradients. Within the TMC, the black region displays the distribution of material 2 (Cu).

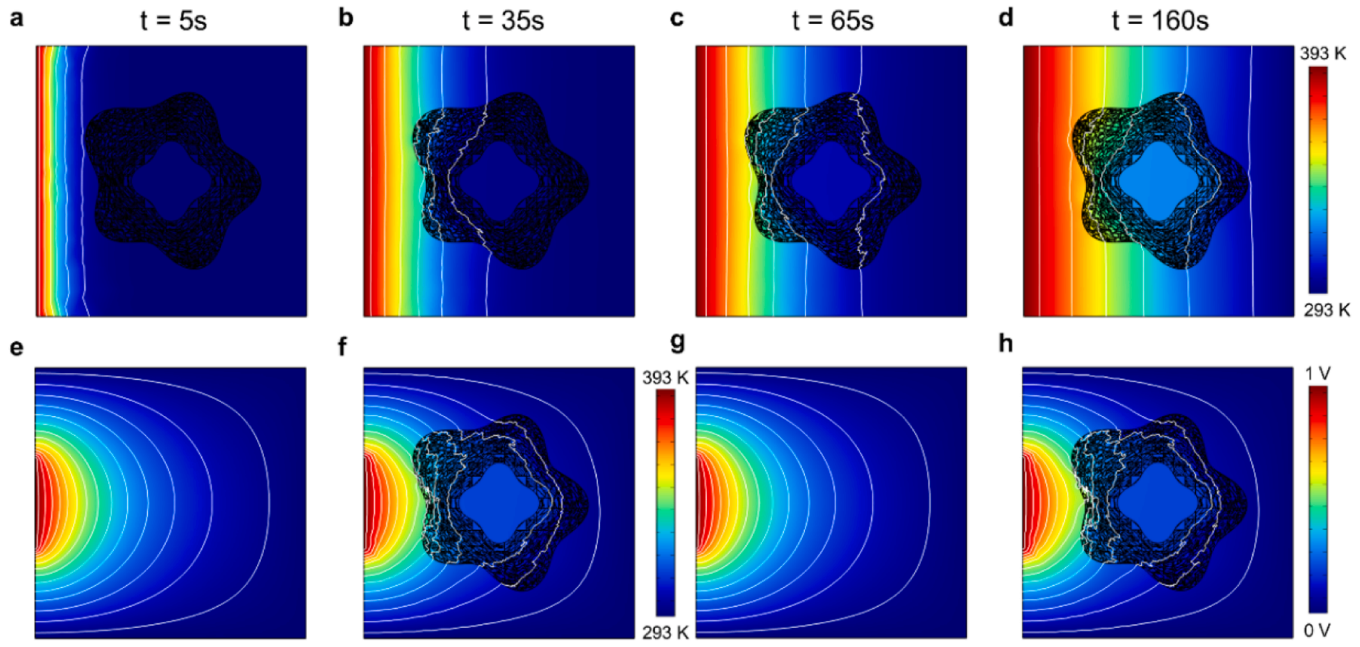


**Fig. 6.** Simulation verifications of the arbitrary-shape multiphysics cloak in the transient case and non-uniform external field. (a)-(d) Transient temperature distribution at different times. (e), (f) Temperature field excited by the non-uniform external field. (g), (h) Potential field excited by the non-uniform external field.

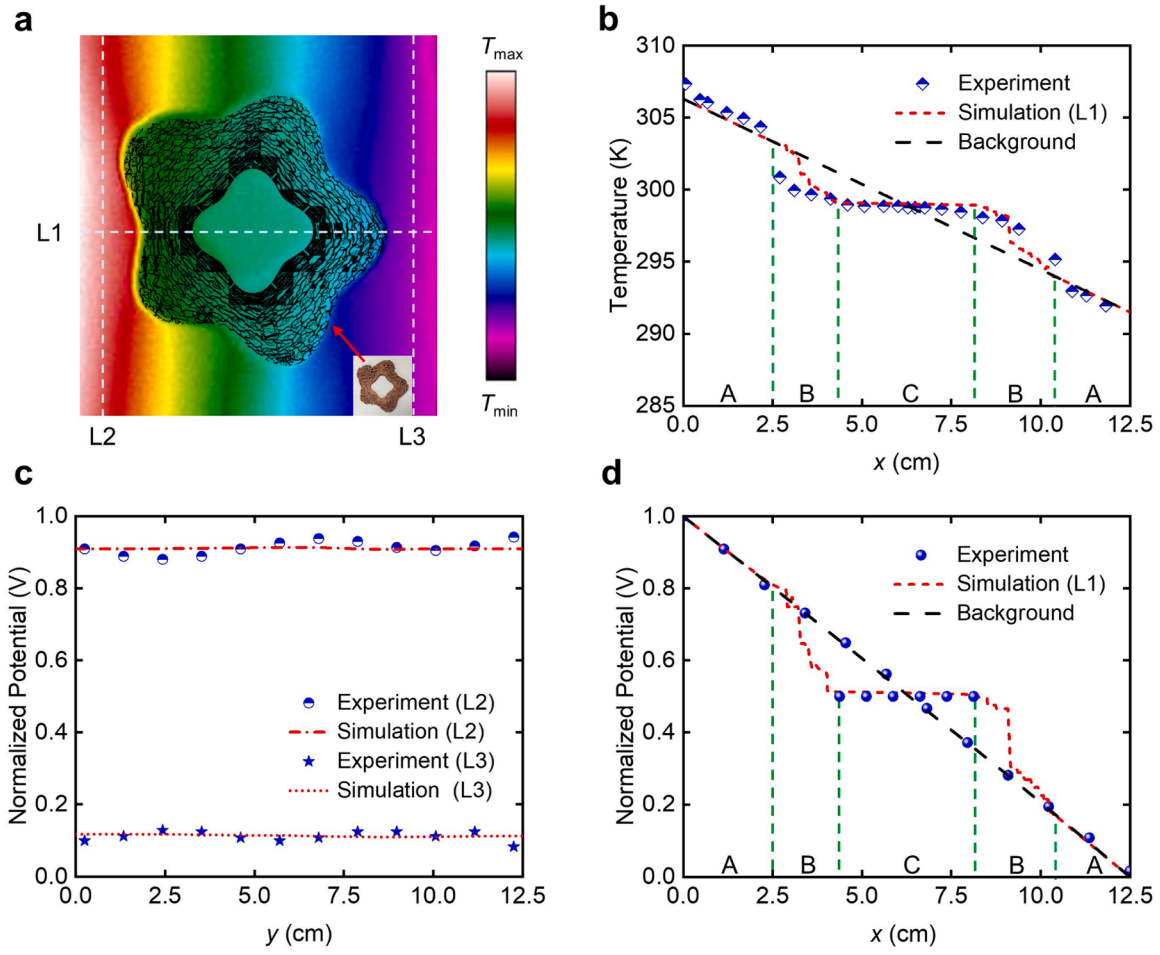


**Fig. 7.** Experimental verifications of the arbitrary-shape multiphysics cloak. (a) The measured temperature field for thermal cloaking. (b) Temperature comparison on line L1. (c) Potential comparison on lines L2 and L3. (d) Potential comparison on line L1.

perform the simulations in the transient case and non-uniform external field, as shown in Fig. 6. From Fig. 6(a)−6(d), the transient temperature/potential distribution always keeps parallel and heat flux/electric current always bypasses the central cloaking region at different times, which illustrates the applicable scenario of TMC is not only limited in steady-state condition. As can been seen in Fig. 6(e)−6(h), excited by the non-uniform external field, the temperature and potential fields keep unchanged and the interior region is cloaked with no heat flux/electric current passing through. All these FEM simulations demonstrate the robustness and powerfulness of the proposed discretion-and-assembly strategy for TMC design and fabrication.

Consistent with the simulation, we fabricate the assembled TMC by 3D printing with 5 mm-thick copper. Then, PDMS is filled into the porous structure of each TFC and solidified with flowing air at room temperature. The background is titanium plate after the process of laser-cutting. To eliminate the influence of the interface between two solid objects, we fill silver adhesive with high thermal ($\kappa = 2.5$ W m$^{-1}$ K$^{-1}$) and electric conductivity ($\sigma = 5 \times 10^4\ \Omega^{-1}$ m$^{-1}$) into the interface. For the thermal cloaking experiment, the heating and Peltier cooling module (DC 24 V) are attached at two sides of the background plate to generate the liner temperature gradient. After the temperature field tends to steady state, we measure the temperature distribution by thermal infrared imager (FLIR SC 620). As shown in Fig. 7a, the temperature field displays perfect thermal cloaking under the liner temperature gradient. To quantitatively analyze the thermal cloaking effect, the horizontal dash line L1 is chosen and the temperature data on L1 in the simulation and experiment are both plotted in Fig. 7b, revealing the agreement between the experimental and simulation results. There is a liner temperature gradient in the exterior zone A, and zero temperature gradient in the interior zone C. Then, the electric cloaking experiment is carried out. A uniform electric bias is applied on the titanium plate through two thin aluminum strips coated on two edges. The potential distributions on the horizontal dash line L1 and vertical dash lines L2 and L3 are measured by high-resolution data acquisition system. The measured potential on the horizontal and vertical dash lines demonstrates the good electric cloaking effect, with parallel external potential field and zero potential gradient in the interior zone C. Therefore, both numerical simulations and experiments indicate that the arbitrary-shape TMC are effective and robust for realizing simultaneous cloaking of heat flux and electric current. The reason why multiphysics cloak based on TFC can achieve good cloaking effect is that each TFC achieves the target anisotropic thermal/electric conductivity and can manipulate heat flux/electric current locally. Since the multiphysics cloak is assembled by millimeter-size TFC with target properties, it advances in stronger local control ability of heat flux/electric current, more flexibility in shape selection and more robustness in different working situations.

In our previous work [40], we proposed and designed transformation multiphysics metamaterials only in theory without experimental validations. However, experimentally fabricating the TFCs and integrating all the TFCs into a single device are rather challenging. To experimentally fabricate, we should take consideration of selecting proper materials, the implementation of stringent anisotropy of effective thermal/electric conductivity, the material connectivity, and microstructure size simultaneously. Through this work, the robustness and feasibility of designing multiphysics metamaterials based on TFCs are validated, which illustrates the design framework of "discretion-and-assembly" strategy and multi-physics topology optimization. Overall, this work focuses on experimental validation of thermal-electric TMC, which may promote the practical application of transformation multiphysics metamaterials.

## 4. Conclusion

In summary, we propose an arbitrary-shape multiphysics cloak which can manipulate heat and electric current simultaneously. Based on multi-physics topology optimization, the desired thermal and electric conductivity can be achieved effectively by designing the distribution of different materials. We numerically and experimentally illustrate that the arbitrary-shape multiphysics cloak is robust for thermal cloaking and electric cloaking in different working cases. The discretion-and-assembly strategy provides great flexibility in terms of shape, functionality and performance robustness, which can be applied to design different metadevices beyond TMC, for instance, transformation multiphysics metamaterials with different functions. Our study offers a general way to design multiphysics metamaterials with target anisotropic properties and the topological-cell-based metamaterials may be applied to couple other multi-physical fields.

## Funding

This work was supported by National Key R & D Project from Ministry of Science and Technology of China (2022YFA1203100), National Natural Science Foundation of China (52076087, 5221150005), Natural Science Foundation of Hubei Province (2023AFA072).

## CRediT authorship contribution statement

**Zhan Zhu:** Writing – review & editing, Writing – original draft, Validation, Methodology, Investigation, Conceptualization. **Zhaochen Wang:** Writing – review & editing, Methodology, Formal analysis. **Tianfeng Liu:** Writing – review & editing, Validation. **Bin Xie:** Methodology, Investigation. **Xiaobing Luo:** Writing – review & editing, Validation, Conceptualization. **Wonjoon Choi:** Writing – review & editing, Writing – original draft, Investigation, Conceptualization. **Run Hu:** Writing – review & editing, Writing – original draft, Validation, Funding acquisition, Conceptualization.

## Declaration of competing interest

The authors declare that they have no known competing financial interests or personal relationships that could have appeared to influence the work reported in this paper.

## Data availability

Data will be made available on request.

## References

[1] J. Pendry, D. Schurig, D.R. Smith, Controlling electromagnetic fields, Science 312 (2006) 1780–1782.
[2] U. Leonhardt, Optical conformal mapping, Science 312 (2006) 1777–1780.
[3] H. Chen, C.T. Chan, Acoustic cloaking in three dimensions using acoustic metamaterials, Appl. Phys. Lett. 91 (2007) 183518.
[4] H. Chen, C.T. Chan, Acoustic cloaking and transformation acoustics, J. Phys. D. Appl. Phys. 43 (2010) 113001.
[5] S.A. Cummer, D. Schurig, One path to acoustic cloaking, New. J. Phys. 9 (2007) 45.
[6] S. Guenneau, C. Amra, D. Veynante, Transformation thermodynamics: cloaking and concentrating heat flux, Opt. Express 20 (2012) 8207–8218.
[7] T. Chen, C.N. Weng, J.S. Chen, Cloak for curvilinearly anisotropic media in conduction, Appl. Phys. Lett. 93 (2008) 114103.
[8] C.Z. Fan, Y. Gao, J.P. Huang, Shaped graded materials with an apparent negative thermal conductivity, Appl. Phys. Lett. 92 (2008) 251907.
[9] R. Hu, W. Xi, Y. Liu, et al., Thermal camouflaging metamaterials, Mater. Today 45 (2021) 120–141.
[10] Y. Li, W. Li, T. Han, et al., Transforming heat transfer with thermal metamaterials and devices, Nat. Rev. Mater. 6 (2021) 488–507.
[11] S. Yang, J. Wang, G. Dai, et al., Controlling macroscopic heat transfer with thermal metamaterials: theory, experiment and application, Phys. Rep. 908 (2021) 1–65.
[12] B. Jenett, C. Cameron, F. Tourlomousis, et al., Discretely assembled mechanical metamaterials, Sci. Adv. 6 (2020) eabc9943.
[13] J. Bauer, L.R. Meza, T.A. Schaedler, et al., Nanolattices: an emerging class of mechanical metamaterials, Adv. Mater. 29 (2017) 1701850.
[14] B. Florijn, C. Coulais, M. Hecke, Programmable mechanical metamaterials, Phys. Rev. Lett. 113 (2014) 175503.
[15] E.M. Dede, F. Zhou, P. Schmalenberg, et al., Thermal metamaterials for heat flow control in electronics, J. Electron. Packag. 140 (2018) 010904–010913.

[16] R. Hu, S. Huang, M. Wang, et al., Binary thermal encoding by energy shielding and harvesting units, Phys. Rev. Appl. 10 (2018) 054032.
[17] S. Narayana, Y. Sato, Heat flux manipulation with engineered thermal materials, Phys. Rev. Lett. 108 (2012) 214303.
[18] R. Schittny, M. Kadic, S. Guenneau, et al., Experiments on transformation thermodynamics: molding the flow of heat, Phys. Rev. Lett. 110 (2013) 195901.
[19] Z. Zhu, X. Ren, W. Sha, et al., Inverse design of rotating metadevice for adaptive thermal cloaking, Int. J. Heat. Mass. Tran. 176 (2021) 121417.
[20] T. Buckmann, M. Kadic, R. Schittny, et al., Mechanical cloak design by direct lattice transformation, Proc. Natl. Acad. Sci. USA 112 (2015) 4930–4934.
[21] L. Wang, J. Boddapati, K. Liu, et al., Mechanical cloak via data-driven aperiodic metamaterial design, Proc. Natl. Acad. Sci. USA 119 (2022) e2122185119.
[22] A. Greenleaf, Y. Kurylev, M. Lassas, et al., Approximate quantum cloaking and almost-trapped states, Phys. Rev. Lett. 101 (2008) 220404.
[23] D.H. Lin, P.G. Luan, Cloaking of matter waves under the global Aharonov-Bohm effect, Phys. Rev. 79 (2009) 051605.
[24] S. Zhang, D.A. Genov, C. Sun, et al., Cloaking of matter waves, Phys. Rev. Lett. 100 (2008) 123002.
[25] C. Lan, K. Bi, X. Fu, et al., Bifunctional metamaterials with simultaneous and independent manipulation of thermal and electric fields, Opt. Express 24 (2016) 23072–23080.
[26] C. Lan, B. Li, J. Zhou, Simultaneously concentrated electric and thermal fields using fan-shaped structure, Opt. Express 23 (2015) 24475–24483.
[27] J.Y. Li, Y. Gao, J.P. Huang, A bifunctional cloak using transformation media, J. Appl. Phys. 108 (2010) 074504.
[28] Y. Ma, Y. Liu, M. Raza, et al., Experimental demonstration of a multiphysics cloak: manipulating heat flux and electric current simultaneously, Phys. Rev. Lett. 113 (2014) 205501.
[29] M. Moccia, G. Castaldi, S. Savo, et al., Independent manipulation of heat and electrical current via bifunctional metamaterials, Phys. Rev. X 4 (2014) 021025.
[30] G. Xu, X. Zhou, Manipulating cell: flexibly manipulating thermal and DC fields in arbitrary domain, Opt. Express 27 (2019) 30819–30829.
[31] L. Zhang, Y. Shi, Bifunctional arbitrarily-shaped cloak for thermal and electric manipulations, Opt. Mater. Express 8 (2018) 2600–2613.
[32] C. Jiang, C. Fang, X. Shen, Multi-physics bi-Functional intelligent meta-device based on the shape memory alloys, Crystals 9 (2019) 438.
[33] P.Y. Chen, J. Soric, A. Alu, Invisibility cloaking: invisibility and cloaking based on scattering cancellation, Adv. Mater. 24 (2012) OP281–OP304.
[34] M. Farhat, S. Guenneau, P.Y. Chen, et al., Scattering cancellation-based cloaking for the Maxwell-Cattaneo heat waves, Phys. Rev. Appl. 11 (2019) 044089.
[35] T. Han, X. Bai, D. Gao, et al., Experimental demonstration of a bilayer thermal cloak, Phys. Rev. Lett. 112 (2014) 054302.
[36] G. Fujii, Y. Akimoto, Optimizing the structural topology of bifunctional invisible cloak manipulating heat flux and direct current, Appl. Phys. Lett. 115 (2019) 174101.
[37] M. Jung, S. Lee, J. Yoo, Bi-objective topology optimization for direct current concentration and heat flux cloaking using adaptive weighting method, Struct. Multidiscip. Optim. 65 (2022) 292.
[38] G. Fujii, Biphysical undetectable concentrators manipulating both heat flux and direct current via topology optimization, Phys. Rev. E. 106 (2022) 065304.
[39] M. Nakagawa, Y. Noguchi, K. Matsushima, et al., Level set-based multiscale topology optimization for a thermal cloak design problem using the homogenization method, Int. J. Heat. Mass. Tran. 207 (2023) 123964.
[40] Z. Zhu, Z. Wang, T. Liu, et al., Field-coupling topology design of general transformation multiphysics metamaterials with different functions and arbitrary shapes, Cell Rep. Phys. Sci. 4 (2023) 101540.
[41] T. Han, P. Yang, Y. Li, et al., Full-parameter omnidirectional thermal metadevices of anisotropic geometry, Adv. Mater. 30 (2018) e1804019.
[42] R. Hu, S. Huang, M. Wang, et al., Encrypted thermal printing with regionalization transformation, Adv. Mater. 31 (2019) e1807849.
[43] R. Hu, S. Zhou, Y. Li, et al., Illusion thermotics, Adv. Mater. 30 (2018) e1707237.
[44] J.C. Kim, Z. Ren, A. Yuksel, et al., Recent advances in thermal metamaterials and their future applications for electronics packaging, J. Electron. Packag. 143 (2021) 010801–010815.
[45] C. Qian, H. Chen, A perspective on the next generation of invisibility cloaks—intelligent cloaks, Appl. Phys. Lett. 118 (2021) 180501.
[46] J.U. Surjadi, L. Gao, H. Du, et al., Mechanical metamaterials and their engineering applications, Adv. Eng. Mater. 21 (2019) 1800864.
[47] E. Andreassen, A. Clausen, M. Schevenels, et al., Efficient topology optimization in MATLAB using 88 lines of code, Struct. Multidiscip. Optim. 43 (2010) 1–16.
[48] W. Sha, M. Xiao, J. Zhang, et al., Robustly printable freeform thermal metamaterials, Nat. Commun. 12 (2021) 7228.
[49] M.P. Bendsøe, O. Sigmund, Topology Optimization: Theory, Methods and Applications, Springer Science & Business Media, 2013.
[50] K. Svanberg, The method of moving asymptotes—a new method for structural optimization, Int. J. Numer. Meth. Eng. 24 (1987) 359–373.